Design, control and pilot study of a lightweight and modular robotic exoskeleton for walking assistance after spinal cord injury

Josep M. Font-Llagunes[1]
Biomechanical Engineering Lab, Department of Mechanical Engineering and Research Centre for Biomedical Engineering, Universitat Politècnica de Catalunya, Diagonal 647, 08028 Barcelona, Spain
josep.m.font@upc.edu

Urbano Lugrís
Laboratory of Mechanical Engineering, University of La Coruña, Mendizábal s/n, 15403 Ferrol, Spain
ulugris@udc.es

Daniel Clos
Biomechanical Engineering Lab, Department of Mechanical Engineering and Research Centre for Biomedical Engineering, Universitat Politècnica de Catalunya, Diagonal 647, 08028 Barcelona, Spain
daniel.clos@upc.edu

F. Javier Alonso
Department of Mechanical, Energetics and Materials Engineering, University of Extremadura, Avda. de Elvas s/n, 06006 Badajoz, Spain
fjas@unex.es

Javier Cuadrado
Laboratory of Mechanical Engineering, University of La Coruña, Mendizábal s/n, 15403 Ferrol, Spain
javier.cuadrado@udc.es

[1] Corresponding author.

ABSTRACT

Walking rehabilitation using exoskeletons is of high importance to maximize independence and improve the general well-being of spinal cord injured subjects. We present the design and control of a lightweight and modular robotic exoskeleton to assist walking in spinal cord injured subjects who can control hip flexion, but lack control of knee and ankle muscles. The developed prototype consists of two robotic orthoses, which are powered by a motor-Harmonic Drive actuation system that controls knee flexion-extension. This actuation module is assembled on standard passive orthoses. Regarding the control, the stance-to-swing transition is detected using two inertial measurement units mounted on the tibial supports, and then the corresponding motor performs a predefined flexion-extension cycle that is personalized to the specific patient's motor function. The system is portable by means of a backpack that contains an embedded computer board, the motor drivers and the battery. A preliminary biomechanical evaluation of the gait-assistive device used by a female patient with incomplete spinal cord injury at T11 is presented. Results show an increase of gait speed (+24.11%), stride length (+7.41%) and cadence (+15.56%) when wearing the robotic orthoses compared to the case with passive orthoses. Conversely, a decrease of lateral displacement of the center of mass (-19.31%) and step width (-13.37% right step, -8.81% left step) are also observed, indicating gain of balance. The biomechanical assessment also reports an overall increase of gait symmetry when wearing the developed assistive device.

1. INTRODUCTION

Spinal cord injury (SCI) is a prevalent impairment in today's society. Every year in the world between 250 000 and 500 000 people suffer this injury; being traffic accidents, falls and violence its three main causes [1]. Inability to walk after SCI decreases patients' quality of life and increases sedentary lifestyle, which in turn lead to other secondary complications like chronic pain, vein thrombosis, urinary tract infections, pressure ulcers or respiratory complications; thereby increasing rates of depression and risk of death as well [2, 3]. Furthermore, SCI carries substantial individual and societal health care costs [1]. In order to improve general well-being and social inclusion of people with SCI, the World Health Organization (WHO) recommends improving access to rehabilitation services and to appropriate assistive devices that enable patients to perform daily living activities like walking, reducing functional limitations and dependency [1]. Gait rehabilitation after SCI has been reported as a high-priority issue for patients independently of their age, time after injury and lesion severity [4, 5]. In addition, recent studies have shown the utility and effectiveness of robotic assistance, in combination with manual therapy, for lower limb motor function recovery through neuronal plasticity after SCI [6].

The current gait assistive robots are either devices that support the user's weight and train walking over a treadmill or foot supports, or exoskeletons that assist over-ground locomotion. Examples of the first kind of robots are Lokomat (Hocoma AG, Switzerland) [7], Gait Trainer GT I (Reha-Stim, Germany) [8, 9], Haptic Walker (Fraunhofer IPK, Germany) [9] and AutoAmbulator (HealthSouth Corporation, USA). These devices are

expensive, bulky and complex to be used, and they are only found in the clinical setting. Examples of the second group of gait trainers are Ekso (Ekso Bionics, USA) [10], ReWalk (ReWalk Robotics, Inc., USA) [11] and Indego (Vanderbilt University, USA) [12]. An extensive literature review on current powered exoskeletons for walking after SCI can be found in [13]. Although exoskeletons are less heavy and costly, they are still out of the reach of the patient, and so, they are principally used in hospitals and rehabilitation centers. Moreover, these robots are used for locomotion rehabilitation during a relatively short period (approximately 8 weeks) as soon as possible after the SCI, and most patients do not receive more physical rehabilitation therapy due to its long-term cost.

Apart from the previous commercial robots, other powered gait-assistive exoskeletal devices have been developed in research labs. There are active ankle-foot orthoses (AFO), which are aimed at assisting the ankle rotation for clinical purposes [14, 15] or to provide push-off assistance during healthy walking [16]. There are also knee exoskeletons or orthoses that provide knee assistance for gait rehabilitation or human performance augmentation [17]. Examples of knee exoskeletons for clinical applications are KNEXO [18], which uses pneumatic artificial muscles as actuators; the knee exoskeleton by Kong et al. [19], which is based on a compact rotary series elastic actuator (cRSEA) using a DC motor; EICOSI [20] and BioKEX [21], which both use direct actuation with a DC motor followed by a transmission mechanism; and AKB [22], which presents a motor and a magnetorheological brake working in parallel that allow energy harvesting through regenerative braking. Knee-ankle-foot orthoses (KAFO) are devices that support both lower limb joints. For instance, the KIT-EXO-1 [23] is a robotic KAFO with two linear

series elastic actuators that control knee and ankle rotations using a force-based approach, and a passive joint that allows foot pronation and supination. One particular type of KAFO, which is particularly well suited for subjects with SCI that can control hip flexion but cannot activate knee muscles, is the stance-control KAFO or SCKAFO [24, 25]. This type of orthosis includes a system to lock the knee rotation during the stance phase, thus avoiding knee flexion and allowing weight bearing during gait. Different typologies of locking systems have been used, e.g., mechanisms that lock rotation at a certain fixed position, electromagnetic wrap-spring clutches, or systems based on friction [24]. Finally, it is worth mentioning the active pelvis orthosis (APO) presented in [26], which is a lightweight bilateral device that employs two series elastic actuators to assist hip flexion-extension.

To assist the gait of patients whose neuromuscular function is affected at all lower limb joints, exoskeletons with actuation up to the hip level are needed. This is the case of HAL (Hybrid Assistive Limb) [27, 28], which is a versatile exoskeleton conceived to assist the gait of people that have suffered stroke or SCI. Another example is LOPES (lower extremity powered exoskeleton) [29], a robot with 8 impedance controlled degrees of freedom (DOF) that actuate pelvis motion and hip and knee rotations over a treadmill using fixed motors and flexible “Bowden cable” transmissions. Finally, H2 [30] is an exoskeleton for over-ground gait training that has the six joints (hip, knee and ankle at both legs) actuated with electrical motors, which are controlled through an impedance control approach.

This work presents the design, control and pilot study of a novel robotic exoskeleton for walking assistance after spinal cord injury, which consists of two separate powered orthoses. The prototype is designed for patients with SCI who are able to control hip flexion, but lack motor control at the knee and ankle joints. The presented device is based on the standard passive orthoses that patients use after rehabilitation at the clinical setting, which include a knee locking system to allow patient's weight bearing during stance and an ankle compliant joint to prevent foot drop. The developed robotic orthosis adds to the passive one two mechatronic modules: a motor-Harmonic Drive actuation system at the knee and an inertial measurement unit (IMU) at the tibial support. The latter serves to detect the user intention to step forward during gait. The main innovations of this system are *lightness*, since it only adds the essential systems to the existing passive orthopedic supports; *modularity*, because the actuation system and the IMU are modular and can be assembled to any orthotic support; and *intuitiveness*, since the user learns how to walk autonomously in cooperation with the device with only a few sessions. Furthermore, the event detection algorithm based on the IMU measurements represents an innovation compared to current exoskeletons, which generally use foot pressure sensors for this purpose.

The objectives of the work are to present the mechanical design and the control architecture of the developed robotic orthosis, and to perform a pilot biomechanical assessment of the walking kinematics of a single patient using that device. Particularly, the kinematics of walking with standard passive orthoses is compared with that obtained using the robotic gait assistive device after six training sessions for adaptation. Patient

kinematics is computed using a state-of-the-art optical motion capture system together with a subject-specific three-dimensional multibody model. In the kinematic analysis, we have investigated gait spatiotemporal parameters and symmetry in those parameters related to right and left lower limbs.

2. ROBOTIC ORTHOSIS DESIGN

The main requirements for the robotic orthosis design are two: 1) to minimally modify the conventional passive supports, so that all components can be mounted on them with low added cost; and 2) to obtain the simplest design possible, yet fully functional for the target patients, regarding actuation and sensing. The developed robotic orthosis has two joints: the knee joint is powered by an electrical motor in series with a Harmonic Drive gearbox (knee actuation system), and the ankle joint is passively actuated by a plastic support to avoid drop-foot walking. This exoskeletal device is intended for over-ground gait assistance either at the clinical center or at patient's home. Preliminary designs of this system were previously reported in [31, 32].

The current device, named ABLE, weights 2.3 kg per leg along with a 1.7 kg backpack containing an ARM-based single board computer BeagleBone Black board (BeagleBoard.org Foundation, Oakland Twp, MI, USA), the motor drivers and the battery. The bilateral tibial and femoral supports are articulated at the knee using a standard revolute joint at the medial side and the motor-gearbox module at the lateral side. Rounded leg braces and velcro straps are used to adjust the orthoses to the lower limb. Foam pads are used to minimize pressures and avoid tissue injuries. Finally, it is important

to highlight that the orthosis structure is custom-made for the patient to avoid the problem of fitting a unique design to the wide range of lower limb morphologies in the SCI population. Fig. 1(a) shows the right orthosis with the knee actuation system and the sensors described in the following subsections.

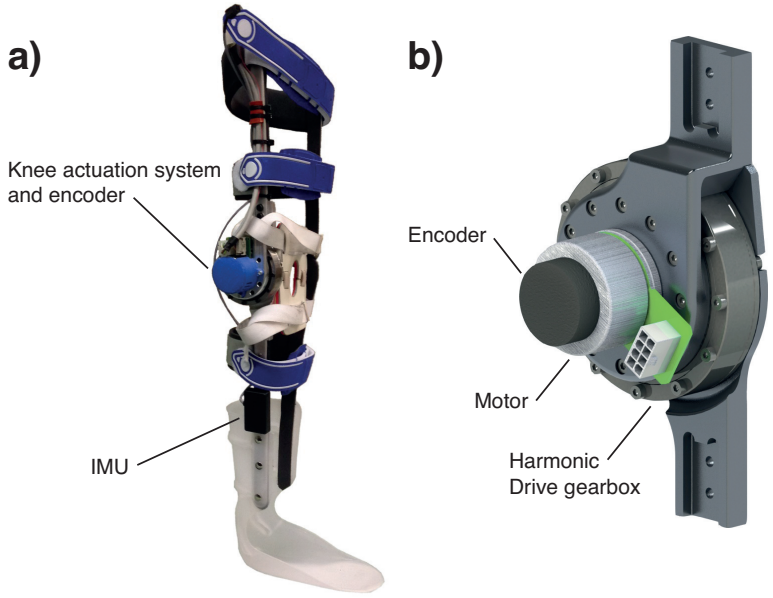

Figure 1. a) General view of the right robotic orthosis of the ABLE exoskeleton showing the knee actuation system and the IMU. b) CAD design of the knee actuation system.

2.1. Knee actuation system

The actuator technologies present in lower limb robotic exoskeletons and orthoses are electric, pneumatic and hydraulic [33]. These actuators might sometimes be used with series or parallel elastic systems for energy efficiency, safety and comfort purposes [26, 34-36]. The design of the knee actuation system and the selection of mechanical components are based on kinematic, dynamic and energetic data (i.e., angular velocity, torque and power) of the knee joint during gait assisted by passive orthoses and crutches

[37]. The main requirements for selecting the actuation system components are high power to weight ratio, reduced system dimensions and good portability of the power supply system (i.e., compact and lightweight).

Based on these criteria, a 70 W brushless DC motor (EC45 flat, Maxon Motor AG, Sachseln, Switzerland) is selected to actuate the knee joint. This motor provides a maximum continuous torque of 128 mNm (nominal torque) when it is powered at 24 V (direct current). In order to increase torque and reduce angular velocity, a Harmonic Drive gearbox (SHD-20-160-2SH, Harmonic Drive AG, Limburg-Lahn, Germany) is coupled to the motor output. We have selected this transmission because it offers a large gear ratio, 160:1 in our case, with a reduced volume. The chosen gear ratio allows to produce a continuous net torque of 20.5 Nm at the gearbox output and instantaneous peak torques of 60 Nm (taking into consideration the motor driver current limit). Fig. 1(b) shows the mechanical design of the knee unit containing the actuation system plus the encoder. To ensure modularity, this unit uses attachments that perfectly fit standard orthopedic braces and supports.

2.2. Control architecture

All the sensors are attached to the orthosis structure to avoid issues related to comfort, safety, reliability and donning/doffing [30]. The sensors used in the prototype are one angular encoder (coupled to the motor) and one IMU per orthosis, Fig. 2. The low-cost 9-DOF IMU (SparkFun Electronics, Niwot, CO, USA) operates at 3.3 V and is placed on the tibial support. The IMU incorporates a triple-axis gyro, a triple-axis accelerometer and a

triple-axis magnetometer. Their outputs are processed by an on-board ATmega328 microcontroller, and orientation and acceleration data are then sent to the BeagleBone Black board through serial interface. A WiFi connection is used to interface the BeagleBone board with an external computer or a smartphone. A graphical user interface (GUI) was built to monitor IMU measurements and to provide controller parameters either using a computer software or a mobile app.

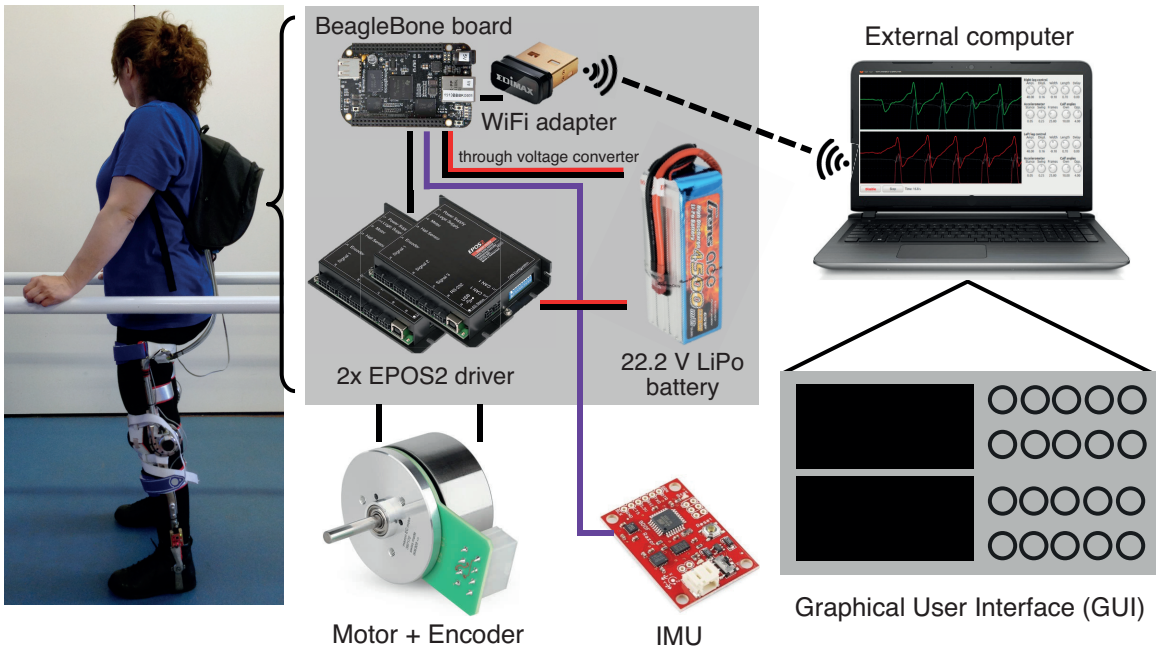

Figure 2. Overall control architecture. The sensors used are one IMU and one angular encoder coupled to the knee motor. A WiFi connection is used to interface with an external computer.

The algorithm to control the two knee motors (right and left) during walking has been implemented in two layers. The outer layer is a swing detection state machine that, based on the IMUs measurements (vertical acceleration and sagittal inclination), identifies the time instant when the knee flexion-extension cycle must be triggered at

initial swing. On the other hand, the inner layer consists of a PID position control with feedforward in velocity and acceleration that keeps the knee in full extension during stance (straight leg, knee locked) and performs a predefined knee flexion-extension trajectory during swing. That trajectory is initiated at the time instant identified by the outer algorithm. Figure 3 presents a block diagram showing the implemented control strategy.

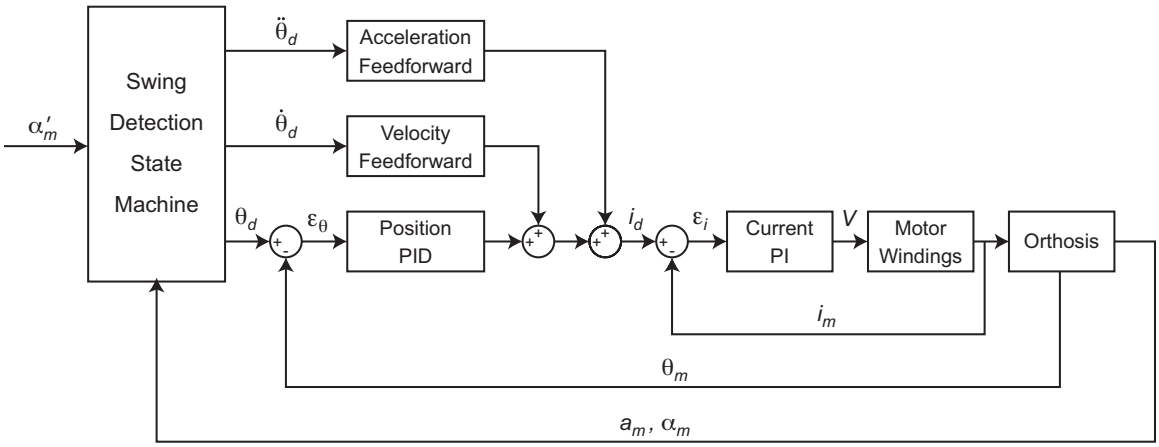

Figure 3. Block diagram of the implemented control strategy. Variables: θ_d stands for the desired knee angle, θ_m stands for the measured knee angle (encoder), ε_θ stands for the knee angle error, i_d stands for the desired current, i_m stands for the measured current, ε_i stands for the current error, V stands for voltage, a_m stands for measured vertical acceleration (IMU), α_m stands for measured shank inclination (IMU), and α'_m stands for the measured shank inclination in the opposite leg (IMU).

2.2.1. Outer layer: swing detection state machine

As said before, each tibial support integrates an IMU that provides its absolute orientation, angular velocity and linear acceleration at a 100 Hz frequency. The algorithm identifies the user intention to swing the leg forward by relying uniquely on the two

inertial measurement units (one per leg). For the sake of safety, the knee flexion-extension cycle of a *certain leg* is only triggered when the next four conditions are all met:

- The vertical acceleration (positive in upward direction) measured at the *same leg* is higher than a trigger value;
- The vertical acceleration measured at the *same leg* has remained below a threshold during a certain time interval;
- The tibial support of the *same leg* has a minimum forward inclination angle;
- The tibial support of the *opposite leg* has a minimum backward inclination angle.

The first condition indicates that the patient has the intention of lifting the leg from the ground to swing it forward. Note that the target patients have this capacity because they preserve motor function at the hip muscles. However, this condition might be fulfilled in other situations apart from the stance-to-swing transition. To ensure a robust detection of that event, the second to fourth conditions have to be met as well at a time. The second condition guarantees that the foot has been in contact with the ground during a certain time, i.e., during stance phase, just before the trigger occurs. Finally, the third and fourth conditions ensure that the posture of the patient is that corresponding to human walking, i.e., the trailing leg leaning forward and the leading leg leaning backward. The latter prevent the knee cycle from being launched if the patient is in standing position and raises a foot.

The threshold values associated to the four conditions above are calibrated for each patient during the adaptation sessions. At the beginning of each session, the patient walks with the knee locked and the IMUs record angular velocity and acceleration data

during walking. Then, the outer layer algorithm is simulated off-line to calibrate the threshold values, so that the swing flexion-extension cycles are launched appropriately.

2.2.2. Inner layer: knee angle control

The knee angle θ is kept equal to zero during stance, so that the joint is locked and the leg straight. Then, once the stance-to-swing transition is detected through the outer algorithm, the knee angle is set to follow a predefined trajectory such that:

$$\theta(t) = \frac{k_a}{2}\left[1 - \cos\left(\frac{2\pi}{t_c}t - \phi(t)\right)\right], \quad 0 \le t \le t_c \tag{1}$$

where k_a stands for the maximum knee flexion angle, t_c is the duration of the cycle, and $\phi(t)$ stands for a time-dependent phase angle that allows tuning the cycle by deforming the shape of the $\theta(t)$ curve:

$$\phi(t) = k_s \sin\left(\frac{\pi}{t_c}t\right) + k_w \sin\left(\frac{2\pi}{t_c}t\right) \tag{2}$$

In Eq. (2), parameter k_s is used to move the peak (maximum flexion) forward or backward in time (Fig. 4(a)), modifying in this way the relative duration of flexion and extension, and parameter k_w is used to increase or decrease the peak width (Fig. 4(b)). The four parameters defining the $\theta(t)$ curve (t_c, k_a, k_s, k_w) can be modified in real time through the developed GUI in order to personalize the knee robotic assistance to the specific walking pattern of the patient. It is important to mention that when defining the parameters for a selected patient, the cycle duration has to be chosen such that swing

flexion-extension ends before the heel-strike of the swinging leg. In such a case, when the flexion-extension cycle finishes the leg is kept fully extended until the next initiation of swing, i.e., terminal swing and stance phase.

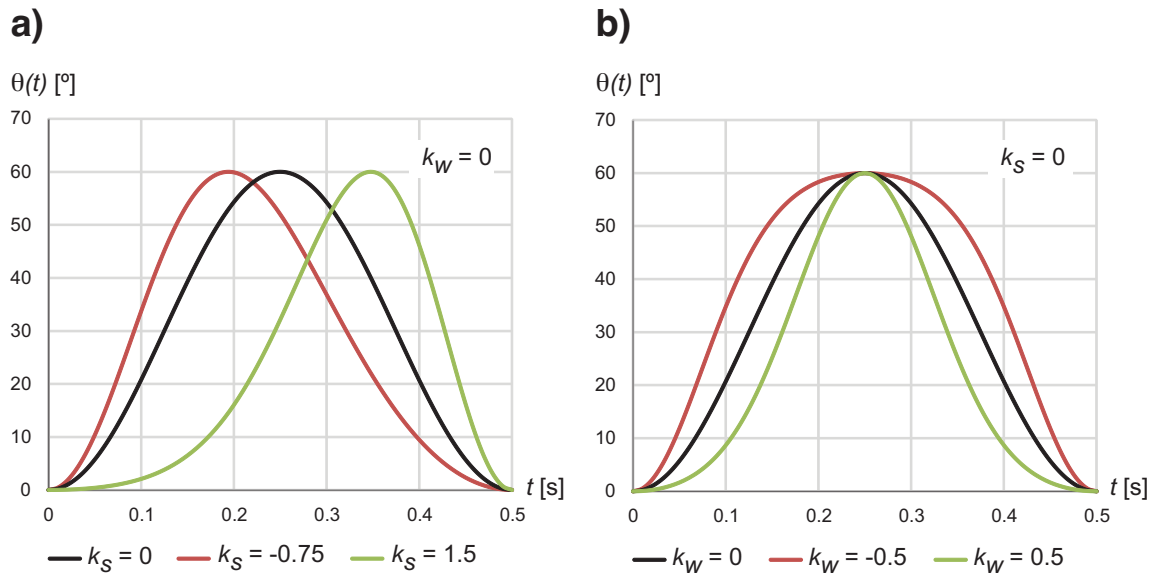

Figure 4. Evolution of $\theta(t)$ versus t for t_c = 0.5 s and k_a = 60°. a) Effect of varying k_s (in rad) with k_w = 0. b) Effect of varying k_w (in rad) with k_s = 0.

2.3. Power supply

The orthosis is powered by a compact lithium polymer (LiPo) battery pack with six cells giving a nominal voltage of 22.2 V (direct current) and a capacity of 4500 mAh. In continuous operation mode, the battery life is approximately 3 hours. As mentioned, the battery pack is placed inside the backpack worn by the subject and it powers two motors, one per leg, the motor drivers plus the BeagleBone board, which is powered with 5 V using an adjustable switching regulator (R-625.0P, RECOM, Gmunden, Austria). The WiFi adapter and the IMUs are directly powered by the BeagleBone.

3. METHODS

In this pilot study, the designed robotic orthoses were tested on a subject with SCI during one session after conducting 6 one-hour training sessions and specific exercises at home. The gait kinematics of the subject with the designed orthoses was compared to the one with the passive conventional orthoses. The Ethics Committee of the University of La Coruña approved all study procedures and the subject gave her informed consent.

3.1. Subject and experimental protocol

The device was tested on an adult female with incomplete SCI at T11 (age: 41 years old, mass: 65 kg, height: 1.52 m). Before the pilot study, the patient was able to walk with her pair of passive KAFO, which included the knee locking mechanism and the compliant plastic support to prevent ankle plantarflexion (foot drop).

In this preliminary evaluation of the gait assistive device two experiments were performed (Test 1 and Test 2). In Test 1, the patient was asked to walk using her pair of passive KAFO with the aid of parallel bars at self-selected speed. After this test, the subject followed six training sessions (one hour of duration per session) wearing the robotic orthoses, in which the maximum knee flexion angle k_a was progressively varied from 0, mimicking the case of wearing passive supports, to 35°. In parallel with these sessions, the patient did specific physical exercises at home to enhance adaptation to the developed device. This training was prescribed by a team of physiotherapists to increase strength in hip flexors and improve adaptation to the device. After this period, a second experiment (Test 2), in which the subject was asked to walk using the robotic orthoses

with the aid of parallel bars at self-selected speed, was performed, Fig. 5(a). In this test, the selected parameters of the inner layer control algorithm were: t_c = 0.56 s, k_a = 35°, k_s = 0.16 rad, k_w = -0.10 rad. In both Test 1 and Test 2, the walking trials were performed under the supervision of engineers and physiotherapists. A questionnaire regarding functional aspects of the device, usability and comfort was provided to the patient after performing Test 2, and its main conclusions are reported in the Discussion session.

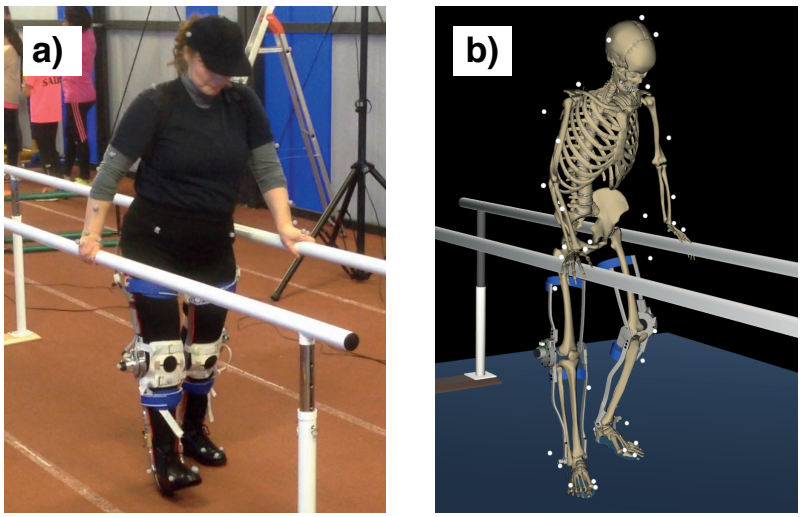

Figure 5. a) Walking test of the subject with SCI assisted by the designed robotic orthoses and using parallel bars (Test 2). b) Subject-specific skeletal model for kinematic analysis of assisted walking.

Four consecutive gait cycles were captured for Test 1 and four more cycles for Test 2 using a state-of-the-art optical motion capture system that measured the three-dimensional position of a set of reflective markers. Then, one average cycle per test was computed with the aim of comparing the walking kinematics in the two cases. A three-dimensional skeletal model was used to determine several spatiotemporal parameters of the subject's gait: gait speed, stride length, cadence, lateral displacement of center of

mass, step width (right and left), leg circumduction (right and left), hip flexion range of motion (right and left), knee flexion range of motion (right and left), and swing phase duration (right and left).

For those parameters related to right and left limbs, a symmetry index (SI) was calculated to account for the gait symmetry during Test 1 and Test 2. This index was calculated according to [38, 39] as:

$$SI(\%) = \frac{X_R - X_L}{0.5(X_R + X_L)} \cdot 100 \tag{3}$$

where X_R and X_L represent a generic gait spatiotemporal parameter for the right and left limb, respectively. In our study, these parameters are step width, leg circumduction, hip flexion ROM and swing phase duration. A symmetry index equal to zero represents symmetry, while a non-zero (positive or negative) index represents asymmetry. The larger its absolute value, the lower the symmetry.

3.2. Three-dimensional skeletal model and signal processing

A subject-specific skeletal model was created to represent the mentioned individual with SCI, Fig. 5(b). In both tests the subject walked on a walkway with parallel bars to keep balance and her motion was captured by 6 optical infrared cameras (OptiTrack Flex:V100, NaturalPoint, Inc., Corvallis, USA) sampling at 100 Hz that computed the position of 37 reflective markers.

The human body was modeled as a three-dimensional multibody system composed by rigid bodies. It consisted of 18 anatomical segments (two hindfeet, two

forefeet, two shanks, two thighs, pelvis, torso, neck, head, two arms, two forearms and two hands) linked by ideal spherical joints, thus defining a model with 57 degrees of freedom (DOF), Fig. 5(b). The global axes were defined as follows: *x*-axis in the posterior-anterior direction, *y*-axis in the medial-lateral direction, and *z*-axis in the vertical direction. The geometric parameters of the model were obtained, for the lower limbs, by applying correlation equations from a reduced set of measurements taken on the subject, following the procedures described in [40]. For the upper part of the body, data from standard tables in [41] were scaled according to the height of the subject. More details about the implementation of this model can be found in [37, 42].

The kinematic information of the motion was obtained from the trajectories of the 37 markers attached to the subject's body (white dots in Fig. 5(b)), which were captured at 100 Hz frequency by means of the 6 infrared cameras. Position data were filtered using an algorithm based on Singular Spectrum Analysis (SSA) [43] and the model coordinates were calculated using algebraic relations. Afterwards, a minimization procedure ensured the kinematic consistency of such coordinates [44]. From that information, the histories of the set of 57 independent coordinates (corresponding to the system's DOF) formed by the Cartesian coordinates of the position vector of the lumbar joint and the 18 x 3 angles that define the absolute orientation of each body, were kinematically obtained and approximated by B-spline curves. Analytical differentiation yielded the corresponding velocity and acceleration histories. More details about the treatment of the captured data can be found in [37].

4. RESULTS OF THE KINEMATIC ANALYSIS

Table 1 shows the previous spatiotemporal parameters for the two averaged gait cycles (Test 1 and Test 2). It is shown that the gait speed in Test 2 increased, mainly due to an increase of walking cadence and stride length in a lower degree. Regarding movement in the frontal plane, the mediolateral displacement of the center of mass (COM) and the step width were reduced in Test 2. Limb circumduction increased for the right limb and decreased for the left limb. As for joint mobility, the hip flexion range of motion (ROM) increased significantly for both legs, and obviously the same happened for the knee joint (which was locked in Test 1). The knee flexion ROM in Test 2 were 37.50° (right) and 33.30° (left). Finally, the swing phase duration was reduced in Test 2, which is consistent with the fact of increased cadence.

Table 1. Computed spatiotemporal parameters in Tests 1 and 2. R stands for right limb and L stands for left limb.

Parameter	**Test 1**	**Test 2**	**% change**
Gait speed (m/s)	0.17	0.21	+24.11
Stride length (m)	0.53	0.57	+7.41
Cadence (step/min)	38.46	44.44	+15.56
COM lateral displacement (cm)	7.89	6.37	-19.31
Step width R (cm)	29.57	25.62	-13.37
Step width L (cm)	27.26	24.86	-8.81
Leg circumduction R (cm)	5.82	6.64	+14.09
Leg circumduction L (cm)	7.87	7.30	-7.16

Hip flexion ROM R (°)	34.32	46.07	+34.22
Hip flexion ROM L (°)	23.41	29.46	+25.84
Swing phase duration R (s)	0.87	0.70	-19.54
Swing phase duration L (s)	1.10	0.80	-27.27

For those gait parameters in Table 1 associated with right and left limbs, the symmetry index SI in Eq. (3) was calculated for Test 1 and Test 2. This index is reported in Table 2. The lower the SI in absolute value, the more symmetric is the gait characteristic. From this table, it can be observed that step width, leg circumduction and swing phase duration became more symmetric when walking with the robotic orthoses. However, even though hip flexion increased in Test 2, this gait parameter is more asymmetric in Test 2. Finally, for the knee flexion ROM in Test 2, SI = +11.88%.

Table 2. Symmetry index (SI) for bilateral parameters in Test 1 and Test 2.

Parameter	**SI in Test 1 (%)**	**SI in Test 2 (%)**
Step width	+8.13	+3.01
Leg circumduction	-29.93	-9.54
Hip flexion ROM	+37.80	+43.97
Swing phase duration	-23.35	-13.33

5. DISCUSSION

This work presents the design concept and functioning of a novel robotic orthosis for walking assistance after spinal cord injury. In particular, this system is intended for

patients that preserve motor function at the hip level. The main advantages of such exoskeleton, compared to the current robotic exoskeletons on the market, are its lightness, modularity and easiness of use. Those advantages come from the fact that instead of building a robotic system from scratch, the device is built over the current passive orthopedic supports that the patient has. Specifically, the knee actuation system and the IMU are mechatronic add-ons directly mounted on the passive supports. By applying this design approach, we intend to improve patient acceptability and reduce time to market. Note that the weight of similar robotic knee exoskeletons for clinical applications range between 2.3 kg and 4.5 kg [17], so our 2.3 kg active KAFO lays in the lower part of this weight range. Moreover, the system is easy to don/doff and to operate through a computer or smartphone interface. Using this interface, the physiotherapist or the user can set the threshold parameters to detect the stance-to-swing transition (outer layer algorithm) and to define the knee flexion-extension desired trajectory (inner layer algorithm). Finally, a unique feature of the presented prototype is its event detection algorithm based solely on IMU measurements. As far as the authors know, this is the only lower limb exoskeleton using this technology to detect gait events.

The patient selected for the preliminary pilot study is a female with incomplete spinal cord injury at T11. The patient showed full engagement and motivation during the tests with the robotic device. The progression during the six training sessions was very satisfactory. At the end of these sessions it became very intuitive for the patient to walk with the robotic orthoses, since the stance-to-swing transition (user intention to step forward) was accurately detected in all steps. Along the sessions, the knee flexion range

of motion was increased from 0 to values around 35°. When asked in the questionnaire about functional aspects of the device, the patient felt her gait was more natural with the robotic orthoses, felt comfortable with the knee flexion assistance, and was also very satisfied with the possibility of adjusting the control parameters independently for each leg. Regarding usability and comfort, the user found correct the weight of the device and the donning/doffing process, and highlighted that it was easy for her to learn how to use the exoskeleton. A less positive aspect was safety, since the patient reported fear for losing balance during walking and suggested the inclusion of an emergency stop button for locking the knees. Other improvements suggested by the user were the elimination of cables from the orthoses to the backpack, the adaptation of the device to other tasks (e.g., sit-to-stand, stair climbing), and the use of more flexible supports to avoid skin injuries due to high pressure. Another interesting aspect arisen by the subject was that the sound of the motor and transmission was positive because she related it to the fact of taking steps.

Regarding the biomechanical assessment of walking with the robotic exoskeleton, as compared to the use of the passive KAFO, results in Table 1 show an increase of stride length (+7.41%) and cadence (+15.56%), resulting in an increase of the gait speed (+24.11%) as well. So, the gait when wearing the presented robotic device is more dynamic than the previous one with the passive supports for the patient at hand. Moreover, the reduction of lateral displacement of the COM (-19.31%) and step width (-13.37% right step, -8.81% left step) indicate gain of balance in the assisted walking. This gain of balance is directly correlated with the knee flexion assistance provided by the

robotic orthosis. Without such assistance (i.e., when wearing the passive KAFO), the lack of knee flexion implies the introduction of body compensatory movements to allow the leg swinging forward, such as hip hiking or circumduction [30, 45]. These movements introduce instability in the walking pattern. Finally, in Table 1 it is also noticeable the increment of hip flexion ROM (+34.22% right step, +25.84% left step), which facilitates the leg swing motion. Note that swing phase duration is reduced for both legs (Table 1), because the overall gait is more dynamic and involves less compensatory movements.

Table 2 shows the results regarding symmetry for the gait parameters commented above. It can be observed that most parameters (step width, circumduction, swing phase duration) are more symmetric in Test 2. Only hip flexion ROM is more symmetric in Test 1, although the two SI values are high for such parameter. Both in Tests 1 and 2, the right hip has significantly more mobility than the left one. We believe that this asymmetry in hip flexion might be reduced with some specific training of the patient's left hip flexor muscles, which still preserve some activity after the injury. To conclude, the gain in symmetry of most analyzed parameters results in a more physiological gait pattern that reduces the risk of suffering secondary musculoskeletal lesions, like hip or shoulder osteoarthritis, as compared to walking with the passive supports.

This study presents some limitations that we should acknowledge here. The first one is related to the fact that only one subject was considered for this pilot study. Therefore, although the results obtained are positive, they must be considered with caution. The authors are planning to conduct a longer study with a larger sample of patients to prove the gait pattern improvements reported above for this pilot case. In

such study, other functional outcome measures (e.g., 10 meter walk test, 6 minute walk test, timed up and go), and clinical scales to assess balance (e.g., Berg balance scale) and motor function will be used to investigate neurorehabilitation after using the robotic orthosis.

Regarding the robotic device, some improvements are envisioned for the near future. After the user comments, it is planned to work on making the device safer. As mentioned above, in the current version the knee motor needs to reach full extension of that joint before heel strike. If that didn't occur, i.e., if the foot contacted the ground before full extension, then there would be the risk that the motor didn't support the patient's weight. To cope with this situation, the authors are working on a newer version with a more powerful motor. Moreover, the incorporation of the emergency stop button suggested by the user is also considered. Other improvements are the miniaturization of the electronics contained in the backpack, and the incorporation of new functionalities to ease the donning/doffing process and to support other tasks like sit-to-stand/stand-to-sit or stair climbing.

6. CONCLUSIONS

This article presents a novel low-cost, lightweight and modular knee-ankle-foot robotic orthosis designed for patients that have suffered a spinal cord injury and preserve hip motor function. The work focuses on the mechanical design of the knee actuation system and the device control system. The knee actuation module is composed of a DC electrical motor and a Harmonic Drive gearbox. On the other hand, the autonomous control

architecture is based on two inertial measurement units to detect the stance-to-swing transition at each step and a PID position control to track a desired knee flexion trajectory during swing (during stance the knee is locked at the full extension position). The system is portable and the user wears a backpack that contains a BeagleBone Black board, the motor drivers and the power supply unit. Furthermore, the device has been thought to be used independently by the patient in a domestic environment and can be operated through a computer interface or a mobile app.

The work reports the findings of a pilot study to evaluate the performance of the developed exoskeletal device on a female subject with incomplete spinal cord injury at T11. In this study, the kinematics of walking using the robotic orthoses was compared to that of walking using standard passive KAFO (with locked knee). In both cases the patient walked with the support of parallel bars. For this study, a full-body patient-specific biomechanical model was developed. Kinematic gait analysis showed that the subject walked faster, more balanced and overall with a more symmetric gait when wearing the developed robotic exoskeleton. While the results obtained through this pilot evaluation were very encouraging, a larger sample of subjects should be analyzed to prove the statistical significance of the found improvements. In such case, functional and clinical outcome measures will also be considered to investigate potential neurorehabilitation after using the device.

As future work, we plan to improve the current device towards the commercial prototype by increasing its robustness, portability and usability. Other future lines of work involve the inclusion of functional electrical stimulation (FES) to the device, to artificially

activate patient's muscles that would cooperate with the robotic actuation, and the use of elasticity in series with the knee actuator to store and release energy during the gait cycle. Finally, the device will also be considered for other patients suffering neurological impairments, such as stroke, traumatic brain injury, cerebral palsy, multiple sclerosis or post-polio syndrome. As in the studied case, preserving hip function will be an inclusion requirement, but the case of unilateral impairments will be considered as well.

ACKNOWLEDGMENT

The authors acknowledge the support of the Spanish Ministry of Economy and Competitiveness (MINECO) along with the European Regional Development Fund (ERDF) under project DPI2015-65959-C3-R, the Galician Government under grant ED431B2016/031, and "la Caixa" Banking Foundation under grant LCF/TR/CI17/10020001.

REFERENCES

[1] Bickenbach, J., Bodine, C., Brown, D., Burns, A., Campbell, R., Cardenas, D., Charlifue, S., Chen, Y., Gray, D., Li, L., Officer, A., Post, M., Shakespeare, T., Sinnott, A., von Groote, P., and Xiong, X., 2013, *International Perspectives on Spinal Cord Injury*, World Health Organization (WHO), Geneva, Switzerland. ISBN: 978-92-4-156466-3

[2] Behrman, A.L., and Harkema, S.J., 2000, "Locomotor training after human spinal cord injury: a series of case studies," Physical Therapy, **80**(7), pp. 688-700. DOI: 10.1093/ptj/80.7.688

[3] Parent, S., Mac-Thiong, J.M., Roy-Beaudry, M., Sosa, J.F., and Labelle, H., 2011, "Spinal cord injury in the pediatric population: a systematic review of the literature," Journal of Neurotrauma, **28**(8), pp. 1515-1524. DOI: 10.1089/neu.2009.1153

[4] Ditunno, P.L., Patrick, M., Stineman, M., and Ditunno, J.F., 2008, "Who wants to walk? Preferences for recovery after SCI: a longitudinal and cross-sectional study," Spinal Cord, **46**(7), pp. 500-506. DOI: 10.1038/sj.sc.3102172

[5] Calhoun, C.L., Schottler, J., and Vogel, L.C., 2013, "Recommendations for mobility in children with spinal cord injury," Topics in Spinal Cord Injury Rehabilitation, **19**(2), pp. 142-151. DOI: 10.1310/sci1902-142

[6] Hubli, M., and Dietz, V., 2013, "The physiological basis of neurorehabilitation – locomotor training after spinal cord injury," Journal of Neuroengineering and Rehabilitation, **10**(5), pp. 1-8. DOI: 10.1186/1743-0003-10-5

[7] Colombo, G., Wirz, M., and Dietz, V., 2001, "Driven gait orthosis for improvement of locomotor training in paraplegic patients," Spinal Cord, **39**(5), pp. 252-255. DOI: 10.1038/sj.sc.3101154

[8] Hesse, S., and Uhlenbrock, D., 2000, "A mechanized gait trainer for restoration of gait," Journal of Rehabilitation Research and Development, **37**, pp. 701-708.

[9] Schmidt, H., Werner, C., Bernhardt, R., Hesse, S., and Krüger, J., 2007, "Gait rehabilitation machines based on programmable footplates," Journal of Neuroengineering and Rehabilitation, **4**(2), pp. 1-7. DOI: 10.1186/1743-0003-4-2

[10] Strickland, E., "Good-bye, wheelchair," IEEE Spectrum, **49**(1), pp. 30-32. DOI: 10.1109/MSPEC.2012.6117830

[11] Esquenazi, A., Talaty, M., Packel, A., and Saulino, M., 2012, "The ReWalk powered exoskeleton to restore ambulatory function to individuals with thoracic-level motor-

complete spinal cord injury," American Journal of Physical Medicine and Rehabilitation, **91**(11), pp. 911-921. DOI: 10.1097/PHM.0b013e318269d9a3

[12] Hartigan, C., Kandilakis, C., Dalley, S., Clausen, M., Wilson, E., Morrison, S., Etheridge, S., and Farris, R., 2015, "Mobility outcomes following five training sessions with a powered exoskeleton," Topics in Spinal Cord Injury Rehabilitation, **21**(2), pp. 93-99. DOI: 10.1310/sci2102-93

[13] Contreras-Vidal, J., Bhagat, N.A., Brantley, J., Cruz-Garza, J.G., He, Y., Manley, Q., Nakagome, S., Nathan, K., Tan, S.H., Zhu, F., and Pons, J.L., 2016, "Powered exoskeletons for bipedal locomotion after spinal cord injury," Journal of Neural Engineering, **13**(3), 031001 1-16. DOI: 10.1088/1741-2560/13/3/031001

[14] Duerinck, S., Swinnen, E., Beyl, P., Hagman, F., Jonkers, I., Vaes, P., and Van Roy, P., 2012, "The added value of an actuated ankle-foot orthosis to restore normal gait function in patients with spinal cord injury: A systematic review," Journal of Rehabilitation Medicine, **44**(4), pp. 299–309. DOI: 10.2340/16501977-0958

[15] Moltedo, M., Bacek, T., Junius, K., Vanderborght, B., and Lefeber, D., 2016, "Mechanical design of a lightweight compliant and adaptable active ankle foot orthosis," *Proc. 6th IEEE International Conference on Biomedical Robotics and Biomechatronics (BioRob)*, Singapore, June 26-29, 2016, pp. 1224-1229. DOI: 10.1109/BIOROB.2016.7523798

[16] van Dijk, W., Meijneke, C., and van der Kooij, H., 2017, "Evaluation of the achilles ankle exoskeleton," IEEE Transactions on Neural Systems and Rehabilitation Engineering, **25**(2), pp. 151–60. DOI: 10.1109/TNSRE.2016.2527780

[17] Chen, B., Zi, B., Wang, Z., Qin, L., and Liao, W.H., 2019, "Knee exoskeletons for gait rehabilitation and human performance augmentation: A state-of-the-art," Mechanism and Machine Theory, **134**, pp. 499-511. DOI: 10.1016/j.mechmachtheory.2019.01.016

[18] Knaepen, K., Beyl, P., Duerinck, S., Hagman, F., Lefeber, D., and Meeusen, R., 2014, "Human–Robot Interaction: Kinematics and Muscle Activity Inside a Powered Compliant Knee Exoskeleton," IEEE Transactions on Neural Systems and Rehabilitation Engineering, **22**(6), pp. 1128-1137. DOI: 10.1109/TNSRE.2014.2324153

[19] Kong, K., Bae, J., and Tomizuka, M., 2012, "A Compact Rotary Series Elastic Actuator for Human Assistive Systems," IEEE/ASME Transactions on Mechatronics, **17**(2), pp. 288-297. DOI: 10.1109/TMECH.2010.2100046

[20] Rifaï, H., Mohammed, S., Hassani, W., and Amirat, Y., 2013, "Nested saturation based control of an actuated knee joint orthosis," Mechatronics, **23**(8), pp. 1141–1149 . DOI:

[21] Liao, Y., Zhou, Z., and Wang, Q., 2015, "BioKEX: A bionic knee exoskeleton with proxy-based sliding mode control," *Proc. IEEE International Conference on Industrial Technology (ICIT)*, Seville, Spain, March 17-19, 2015, pp. 125-130. DOI: 10.1016/j.mechatronics.2013.09.007

[22] Ma, H., Chen, B., Qin, L., and Liao, W.H., 2017, "Design and testing of a regenerative magnetorheological actuator for assistive knee braces," Smart Materials and Structures, **26**(3), pp. 1-13 . DOI: 10.1088/1361-665X/aa57c5

[23] Beil, J., Perner, G., and Asfour, T., 2015, "Design and control of the lower limb exoskeleton KIT-EXO-1," *Proc. IEEE International Conference on Rehabilitation Robotics*, Singapore, August 11-14, 2015, pp. 119-124. DOI: 10.1109/ICORR.2015.7281186

[24] Yakimovich, T., Lemaire, E.D., and Kofman, J., 2009, "Engineering desing review of stance-control knee-ankle-foot orthoses," Journal of Rehabilitation Research and Development, **46**(2), pp. 257-267.

[25] Shamaei, K., Napolitano, P.C., and Dollar, A.M., 2014, "Design and Functional Evaluation of a Quasi-Passive Compliant Stance Control Knee–Ankle–Foot Orthosis," IEEE Transactions on Neural Systems and Rehabilitation Engineering, **22**(2), pp. 258-268. DOI: 10.1109/TNSRE.2014.2305664

[26] Giovacchini, F., Vannetti, F., Fantozzi, M., Cempini, M., Cortese, M., Parri, A., Yan, T., Lefeber, D., and Vitiello, N., 2015, "A light-weight active orthosis for hip movement assistance," Robotics and Autonomous Systems, **73**, pp. 123-134. DOI: 10.1016/j.robot.2014.08.015

[27] Nilsson, A., Vreede, K.S., Häglund, V., Kawamoto, H., Sankai, Y., and Borg, J., 2014, "Gait training early after stroke with a new exoskeleton – the hybrid assistive limb: a study of safety and feasibility", Journal of Neuroengineering and Rehabilitation, **11**(92), pp. 1-10. DOI: 10.1186/1743-0003-11-92

[28] Tsukahara, A., Hasegawa, Y., Eguchi, K., and Sankai, Y., 2015, "Restoration of gait for spinal cord injury patients using HAL with intention estimator for preferable swing speed," IEEE Transactions on Neural Systems and Rehabilitation Engineering, **23**(2), pp. 308-318. DOI: 10.1109/TNSRE.2014.2364618

[29] Veneman, J.F., Kruidhof, R., Hekman, E.E.G., Ekkelenkamp, R., Van Asseldonk, E.H.F., and Van der Kooij, H., 2007, "Design and evaluation of the LOPES exoskeleton robot for interactive gait rehabilitation," IEEE Transactions on Neural Systems and Rehabilitation Engineering, **15**(3), pp. 379-386. DOI: 10.1109/TNSRE.2007.903919

[30] Bortole, M., Venkatakrishnan, A., Zhu, F., Moreno, J.C., Francisco, G.E., Pons, J.L., and Contreras-Vidal, J.L., 2015, "The H2 robotic exoskeleton for gait rehabilitation after

stroke: early findings from a clinical study," Journal of Neuroengineering and Rehabilitation, **12**(54), pp. 1-14. DOI: 10.1186/s12984-015-0048-y

[31] Font-Llagunes, J.M., Pàmies-Vilà, R., Alonso, J., and Lugrís, U., 2011, "Simulation and design of an active orthosis for an incomplete spinal cord injured subject," Procedia IUTAM, **2**, pp. 68-81. DOI: 10.1016/j.piutam.2011.04.007

[32] Font-Llagunes, J.M., Lugrís, U., Romero, F., Clos, D., Alonso, F.J., and Cuadrado, J., 2014, "Design of a patient-tailored active knee-ankle-foot orthosis to assist the gait of spinal cord injured subjects," *Proc. International Workshop on Wearable Robotics (WeRob)*, Baiona, Spain, September 14-19, 2014, paper 54.

[33] Hong, Y.W., King, Y.J., Yeo, W.H., Ting, C.H., Chuah, Y.D., Lee, J.V., and Chok, E.T., 2014, "Lower extremity exoskeleton: Review and challenges surrounding the technology and its role in rehabilitation of lower limbs," Australian Journal of Basic and Applied Sciences, **7**(7), pp. 520-524.

[34] Vallery, H., Veneman, J., van Asseldonk, E., Ekkelenkamp, R., Buss, M., and van der Kooij, H., 2008, "Compliant actuation of rehabilitation robots," IEEE Robotics and Automation Magazine, **15**(3), pp. 60-69. DOI: 10.1109/MRA.2008.927689

[35] Vanderborght, B., Van Ham, R., Lefeber, D., Sugar, T.G., and Hollander, K.W., 2009, "Comparison of mechanical design and energy consumption of adaptable, passive-compliant actuators," International Journal of Robotics Research, **28**(1), pp. 90-103. DOI: 10.1177/0278364908095333

[36] Bae, J., Kong, K., and Tomizuka, M., 2011, "Gait phase-based control for a rotary series elastic actuator assisting the knee joint," Journal of Medical Devices 5 (031010) (2011) 1-6. DOI: 10.1115/1.4004793

[37] Lugrís, U., Carlín, J., Luaces, A., and Cuadrado, J., "Gait analysis system for spinal cord injured subjects assisted by active orthoses and crutches," Journal of Multi-body Dynamics, **227**(4), pp. 363-374. DOI: 10.1177/1464419313494935

[38] Robinson, R.O., Herzog, W., and Nigg, B.M., 1987, "Use of force platform variables to quantify the effects of chiropractic manipulation on gait symmetry," Journal of Manipulative and Physiological Therapeutics, **10**, pp. 172-176.

[39] Sadeghi, H., Allard, P., Prince, F., and Labelle, H., 2000, "Symmetry and limb dominance in able-bodied gait: a review," Gait and Posture, **12**, pp. 34-45. DOI: 10.1016/S0966-6362(00)00070-9

[40] Vaughan, C.L., Davis, B.L., and O'Connor, J.C., 1999, *Dynamics of Human Gait*, 2nd ed., Kiboho Publishers, Cape Town, South Africa. ISBN: 0-620-23558-6

[41] Ambrosio, J.A.C., and Kecskemethy, A., 2007, "Multibody dynamics of biomechanical models for human motion via optimization," Multibody Dynamics. Computational Methods and Applications (Garcia Orden, J.C., Goicolea, J.M., and Cuadrado, J., Eds.), pp. 245-270. DOI: 10.1007/978-1-4020-5684-0_12

[42] Lugrís, U., Carlín, J., Pàmies-Vilà, R., Font-Llagunes, J.M., and Cuadrado, J., 2013, "Solution methods for the double-support indeterminacy in human gait," Multibody System Dynamics, **30**(3), pp. 247-263. DOI: 10.1007/s11044-013-9363-x

[43] Golyandina, N., Nekrutkin, V., and Zhigljavsky, A., 2001, *Analysis of Time Series Structure: SSA and Related Techniques*, Chapman & Hall/CRC, Washington, DC. ISBN: 1-58488-194-1

[44] Alonso, F.J., Cuadrado, J., Lugrís, U., and Pintado, P., 2010, "A compact smoothing–differentiation and projection approach for the kinematic data consistency of biomechanical systems," Multibody System Dynamics, **24**(1), pp. 67-80. DOI: 10.1007/s11044-010-9191-1

[45] Pietrusinski, M., Cajigas, I., Severini, G., Bonato, P., and Mavroidis, C., 2014, "Robotic gait rehabilitation trainer," IEEE/ASME Transactions on Mechatronics, **19**(2), pp. 490-499. DOI: 10.1109/TMECH.2013.2243915

Figure Captions List

Fig. 1 [page 8] a) General view of the right robotic orthosis of the ABLE exoskeleton showing the knee actuation system and the IMU. b) CAD design of the knee actuation system.

Fig. 2 [page 10] Overall control architecture. The sensors used are one IMU and one angular encoder coupled to the knee motor. A WiFi connection is used to interface with an external computer.

Fig. 3 [page 11] Block diagram of the implemented control strategy. Variables: θ_d stands for the desired knee angle, θ_m stands for the measured knee angle (encoder), ε_θ stands for the knee angle error, i_d stands for the desired current, i_m stands for the measured current, ε_i stands for the current error, V stands for voltage, a_m stands for measured vertical acceleration (IMU), α_m stands for measured shank inclination (IMU), and α'_m stands for the measured shank inclination in the opposite leg (IMU).

Fig. 4 [page 14] Evolution of $\theta(t)$ versus t for t_c = 0.5 s and k_a = 60°. a) Effect of varying k_s (in rad) with k_w = 0. b) Effect of varying k_w (in rad) with k_s = 0.

Fig. 5 [page 16] a) Walking test of the subject with SCI assisted by the designed robotic orthoses and using parallel bars (Test 2). b) Subject-specific skeletal model for kinematic analysis of assisted walking.

Table Caption List